Journal of Colloid and Interface Science 354 (2011) 116–123

Contents lists available at ScienceDirect

Journal of Colloid and Interface Science

www.elsevier.com/locate/jcis

Curcumin-loaded PLGA-PEG-PLGA triblock copolymeric micelles: Preparation, pharmacokinetics and distribution in vivo

Zhimei Song [a,b,1], Runliang Feng [b,1], Min Sun [a], Chenyu Guo [a], Yan Gao [a], Lingbing Li [a], Guangxi Zhai [a,*]

[a] Department of Pharmaceutics, College of Pharmacy, Shandong University, 44 Wenhua Xilu, Jinan 250012, China
[b] Department of Pharmaceutical Engineering, College of Medicine and Life Science, University of Jinan, Jinan 250022, China

ARTICLE INFO

Article history:
Received 4 August 2010
Accepted 11 October 2010
Available online 16 October 2010

Keywords:
PLGA-PEG-PLGA micelle
Curcumin
Pharmacokinetics
Biodistribution

ABSTRACT

The aim of this study was to assess the potential of new copolymeric micelles to modify the pharmacokenetics and tissue distribution of Curcumin (CUR), a hydrophobic drug. In the present study, a poly (D,L-lactide-co-glycolide)-b-poly(ethylene glycol)-b-poly(D,L-lactide-co-glycolide) (PLGA-PEG-PLGA) copolymer was synthesized and characterized by ^{1}H NMR, gel permeation chromatography and FTIR analysis. The CUR-loaded PLGA-PEG-PLGA micelles were prepared by dialysis method and the physicochemical parameters of the micelles such as zeta potential, size distribution and drug encapsulation were characterized. The pharmacokinetics and biodistribution of CUR-loaded micelles in vivo were evaluated. The results showed that the zeta potential of CUR-loaded micelles was about −0.71 mV and the average size was 26.29 nm. CUR was encapsulated into PLGA-PEG-PLGA micelles with loading capacity of 6.4 ± 0.02% and entrapment efficiency of 70 ± 0.34%. The plasma $AUC_{(0-\infty)}$, $t_{1/2\alpha}$, $t_{1/2\beta}$ and MRT of CUR micelles were increased by 1.31, 2.48, 4.54 and 2.67 fold compared to the CUR solution, respectively. The biodistribution study in mice showed that the micelles decreased drug uptake by liver and spleen and enhanced drug distribution in lung and brain. These results suggested that PLGA-PEG-PLGA micelles would be a potential carrier for CUR.

1. Introduction

Recently, medical applications of polymeric nanoparticles to achieve site-special drug delivery have attracted growing interest. Especially, polymeric micelles are currently recognized as one of the most promising carriers of drug [1]. Amphiphilic copolymer in aqueous solution can self- assemble into micelles due to hydrophobic interactions among the water-insoluble segments. Polymeric micelles as nanocarriers have gained attention due to several advantages, such as (i) the low toxicity; (ii) the high stability; and (iii) the small size (<200 nm), which has made them ideal candidate for passive targeting of solid tumor by enhanced permeation and retention (EPR) effect [2–5]. This approach has been used to deliver drugs such as paclitaxel [6], prednisone acetate [7] and doxorubicin [8], etc.

Copolymer PLGA-PEG-PLGA is an excellent biomedical material and displays many advantages, e.g. biocompatible, degradable, thermosensitive and easy controlled characters. Potential advantage provided by the hydrophilic poly (ethylene glycol) (PEG) can improve the biocompatibility of the delivery vehicle. This is because most of the biological environment is hydrophilic in nature and biocompatibility appears to be correlated directly with the degree of hydrophilicity that a surface exhibits [9]. The nonionic hydrophilic PEG shell can suppress the adsorption of opsonin and subsequent clearance by the mononuclear phagocyte system, prolong the circulation time, and influence the pharmacokinetics and biodistribution of the drug delivery system [10,11], while the hydrophobic core of D,L-lactide (D,L-LA) and glycolide (GA) can solubilize hydrophobic drugs. Hence, it has been studied widely as a biomaterial for sustained release of drugs and antigens [12–18]. But there is rare report about PLGA-PEG-PLGA nano-micelles as carriers for drug delivery. Many early reports have proved that polymeric amphiphiles consisting of hydrophilic PEG and hydrophobic low-molecular-weight natural components such as diacyllipid, fatty acid and bile salts can form self-aggregated micelles [19–22]. It is therefore conceivable that the triblock copolymer PLGA-PEG-PLGA formed by incorporation of a hydrophilic segment such as PEG into the hydrophobic PLGA chain would self-assemble into micelles and facilitate the drug release.

Curcumin (diferuloylmethane, CUR, Fig. 1) is a low-molecular-weight, natural polyphenolic compound that is isolated from the rhizome of turmeric (*Curcuma longa*). It is a lipophilic fluorescent molecule with phenolic groups and conjugated double bonds. It has a low intrinsic toxicity but a wide range of pharmacological activities including antioxidant, anti-inflammatory, antimicrobial,

* Corresponding author. Address: Department of Pharmaceutics, College of Pharmacy, Shandong University, 44 Wenhua Xilu, Jinan 250012, China.
E-mail address: professorgxzhai@yahoo.cn (G. Zhai).
[1] These authors Contributed equally to the work.

0021-9797/$ - see front matter © 2010 Elsevier Inc. All rights reserved.
doi:10.1016/j.jcis.2010.10.024

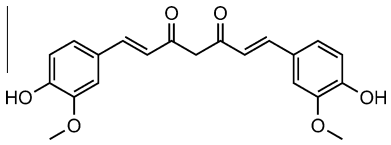

Fig. 1. Structure of curcumin (CUR).

antiamyloid, and antitumor properties [23,24]. Preclinical studies of CUR have shown its ability to inhibit carcinogenesis in a variety of cell lines that include breast, cervical, colon, gastric, hepatic, leukemia, oral epithelial, ovarian, pancreatic, and prostate cancer [25]. The ability of CUR to induce apoptosis in cancer cells without cytotoxic effects on healthy cells makes it a potential compound for drug development against cancer [25,26].

The major problem with CUR is its extremely low solubility in aqueous solution (2.99×10^{-8} M) and its poor bioavailability, which limits its clinical efficacy [27,28]. Attempts have been made through encapsulation in polymeric micelles, liposomes, polymeric nanoparticles, lipid-based nanoparticles, and hydrogels to increase its aqueous solubility and bioavailability [29–34].

In this study, the PLGA-PEG-PLGA conjugate was synthesized through an ester linkage ring-opening reaction with Stannous 2-ethylhexanoate as catalysis. The micelles of PLGA- PEG-PLGA were successfully prepared at first. The physicochemical characteristics of CUR-loaded PLGA-PEG-PLGA micelles such as morphology, particle size, zeta potential and loading efficiency were investigated. And the pharmacokinetics and biodistribution of CUR-loaded micelles in mice were evaluated with CUR solution (CUR-solution) as control.

2. Experimental section

2.1. Materials

CUR was purchased from Fluka Chemical Company Inc. (Buchs, Switzerland). Poly (ethylene glycol) (PEG) ($\overline{Mw} = 1500$) was purchased from Shanghai Pudong Gaonan Chemical Factory (Shanghai, China). D,L-Lactide, and glycolide monomers for synthesis of PLGA–PEG–PLGA polymer were obtained from Jinan Daigang Biotechnology Co., Ltd. (Jinan, China). Stannous 2-ethylhexanoate was procured from Sigma Chemicals (St. Louis, MO, USA). Pyrene was obtained from Baotou Science and Technology Industry Trade Co. Ltd. (Baotou, China). All the other chemicals and solvents were of analytical grade or higher, obtained commercially. Dialysis membrane was obtained from Viskase® Companies, Inc. (USA).

2.2. Synthesis of PLGA-PEG-PLGA triblock copolymer

PLGA-PEG-PLGA was synthesized by ring-opening method described by Ali et al. [35]. Briefly, ring-opening polymerization of lactide (5905 mg) and glycolide (595 mg) in the presense of PEG (3500 mg) was performed to synthesize PLGA-PEG-PLGA using stannous octanate as catalyst.

2.3. Polymer characterization

2.3.1. ^1H NMR spectrum of copolymer

^{1}H NMR spectrum has been used for structure analysis. Spectra were recorded using a 600 MHz Bruker spectrometer (AVANCE model, Germany) at 25 °C. Deuterated chloroform ($CDCl_3$) was used as solvent.

2.3.2. FTIR analysis

The characterization of the functional groups was carried out by FTIR analysis using a NEXUS 470 FTIR spectroscopy (Nicolet, USA). The samples were prepared by spreading PLGA-PEG-PLGA on the potassium bromide tablet or compressing LA, GA and PEG into pellets with potassium bromide.

2.3.3. Gel permeation chromatography

Copolymer molecular weights were determined on a Waters GPC system equipped with an isocratic pump (Waters 1525) operated at a flow rate of 1.0 mL/min with tetrahydrofuran (THF), an autosampler (Waters 717 plus), a column oven and a dual λ absorbance detector (Waters 2487) with integrated temperature controller maintained at 35 °C. For molecular mass separation a guard column (PLgel 5 μm) and a Styragel HT3 column (10 μm, 300 × 7.5 mm) were used in-line at 35 °C. Calibration was carried out using ND (narrow distributed)-polystyrene standards. The mobile phase was THF (HPLC grade) stabilized with dieter butyl-2,6-methyl-4-phenol. Polymer sample was dissolved in THF, shortly sonicated in an ultrasonic bath to form a homogenous solution. Chromatography was carried out after sample filtration through a 0.45 μm PTFE filter.

2.4. Physicochemical characterization of copolymer micelles

2.4.1. CMC of copolymer

Copolymer was precisely weighted and dissolved in redistilled water at 5–8 °C and stored at 4 °C for 24 h. By dilution with redistilled water, a series of aqueous solutions with different concentration of copolymer were obtained as follow: 1×10^{-3}, 5×10^{-4}, 1×10^{-4}, 5×10^{-5}, 1×10^{-5}, 5×10^{-6}, 1×10^{-6}, 5×10^{-7}, 1×10^{-7}, 5×10^{-8} g/mL.

A 0.1 mL of 2×10^{-4} mol/L solution of pyrene in acetone was aliquoted into a series of amber glass vials and acetone was evaporated under a stream of nitrogen. The copolymer solutions in water ranging in concentrations were added into the vials to give a final pyrene concentration of 2×10^{-6} mol/L All the solutions were equilibrated in water bath at 60 °C, stored overnight at room temperature and filtered through 0.45 μm filter membrane prior to measurements.

CMC of the copolymer was determined by fluorescence spectroscopy using pyrene as fluorescence probe. The fluorescence spectrum was recorded on a fluorescence spectrophotometer (F-7000 FL, Hitachi Corp., Japan). The excitation spectrum was recorded from 300 to 360 nm with an emission wavelength of 390 nm. Both excitation and emission bandwidths were 2.5 nm. Scanning speed was 240 nm min^{-1}. Fluorescent spectra of pyrene solutions contained a vibration band exhibiting high sensitivity to the polarity of the pyrene environment. As shown in the excitation spectra of pyrene with formation of micelles, pyrene would move into the inside of micelles from the aqueous phase, which resulted in an alteration in the intensity ratio (I_{335}/I_{332}) of pyrene fluorescence bands A (335 nm) to B (332 nm). The intensity ratios (I_{335}/I_{332}) were analyzed as a function of copolymer concentration at room temperature. A CMC value was taken from the intersection of the tangent to the curve at the inflection with the horizontal tangent through the points at low concentrations.

2.4.2. Encapsulation of CUR in PLGA-PEG-PLGA micelles

The micelles were prepared by a solvent-dialysis method. Briefly, the copolymer (50 mg) and CUR (5 mg) were dissolved in 2 mL of acetone, and treated with ultrasonic for 5 min. The mixture was then dialyzed against distilled water at 4–8 °C for 24 h using a dialysis membrane with a molecular weight cut-off of 3500. After dialysis, the solution in the dialysis bag was collected and filtered with 0.45 μm pore-sized membrane to remove the undissolved CUR.

2.4.3. Particle size and zeta potential

The mean diameter and zeta potential of the CUR-loaded copolymer micelles were determined by using a Zetasizer 3000HS instrument (Malvern Instruments Ltd., UK). The dimension of the micelles without curcumin was also characterized, The measurements were performed using He–Ne Laser beam of 633 nm wavelength. Particle size was measured at a fixed scattering angle of 90° at 25 °C, and the data were evaluated using the volume distribution. Zeta potential was analyzed at 25 °C. All the measurements were analyzed in triplicate.

2.4.4. Morphology of copolymer micelle

The morphology of the copolymer micelles was observed under transmission electron microscope (TEM, JEM-1200EX, JEOL, Tokyo, Japan). One drop of copolymeric micelle solution was placed on a film-coated copper grid followed by negative staining with phosphotungstic acid (PTA) for 20 s, excess solution was absorbed with filter paper, and samples were naturally dried for observation.

2.4.5. Entrapment efficiency (EE) and drug loading (DL)

The CUR content in the micelles was determined using the UV–vis spectrophotometer at 425 nm. The drug loading content and drug encapsulation efficiency were calculated based on the following formula [36]:

$$\text{encapsulation efficiency} = \frac{\text{weight of drug in micelles}}{\text{weight of the initial drug}} \times 100\%$$

$$\text{drug loading content} = \frac{\text{weight of drug in micelles}}{\text{weight of micelles}} \times 100\%$$

Because of CUR's low solubility in water (11 ng/ml) [30,31], its content in water was ignored when compared with loading content of CUR into the micelles. So the content of free CUR in water was not included when calculating the loading content and entrapment efficiency.

2.5. Evaluation of the pharmacokinetics and biodistribution in mice of CUR-loaded copolymer micelles following i.v. administration

Kunming mice with body weights ranging from 18 to 22 g were purchased from Experimental Animal Center of Shandong University (Shandong, China). All animal experiments complied with the requirements of the National Act on the use of experimental animals (People's Republic of China). Mice were fasted for 12 h before experiment with free access to water. They were randomly divided into two groups with five for each group.

As control, CUR was solubilized in a reported solution for injection containing 15% of DMA, 45% of PEG400 and 40% of dextrose solution with the concentration of dextrose at 5% [37]. Control solution and CUR-loaded copolymer micelles were injected intravenously to the mice via the tail vein at the doses of 10 mg/kg, respectively. At each time point blood samples were collected *via* eye sockets and immediately centrifuged at 3000 r/min for 10 min to obtain plasma. The animals were sacrificed ($n = 5$) by cervical dislocation. Tissue samples (i.e. heart, lung, kidney, liver, brain and spleen) were collected. These tissue samples (no more than 100 mg) were washed with ice-cold saline, blotted with filter paper, to remove fluid, weighed, then placed in 1 mL physiological saline and homogenized. 50 μL of citrate buffer solution were added to 0.8 mL of aliquots of the homogenized samples or 150 μL of plasma, and vortexed for 30 s, followed by addition of 2 mL of ethyl acetate, respectively. The above mixture was vortexed for 3 min and centrifugated for 5 min at 3000 r/min, respectively. The supernatant was collected and transferred to other centrifuge tubes, the residue was added 2 mL of ethyl acetate again. The combined supernatant (containing extracts) was dried under a stream of nitrogen gas at 40 °C. The obtained solid samples were re-dissolved with methanol (100 μL) and centrifuged at 10,000 r/min for 10 min. 20 μL of supernatant was collected and detected by high performance liquid chromatography (HPLC).

CUR was assayed by reversed phase-HPLC with UV detector (Agilent 1100, USA) [37]. The mobile phase was composed of 52% acetonitrile and 48% citric buffer (1% w/v citric acid solution adjusted to pH 3.0 using concentrated sodium hydroxide solution). The flow rate was set at 1.0 mL/min and the detection wavelengths were at 425 nm.

3. Results and discussion

3.1. Polymer characterization

The structure of PLGA-PEG-PLGA was shown in Fig. 2. It is a nonionic triblock copolymer consisting of hydrophilic PEG and hydrophobic PLGA segments.

A typical ^{1}H NMR spectrum of PLGA-PEG-PLGA obtained was very similar to the reported spectrum [38]. The presence of methine (CH) and methyl (CH_3) protons in LA were observed at around 5.17 ppm (e) and 1.55 ppm (a), respectively. Tetralet and doublet split peaks were obviously found. The methene protons in CH_2 group of PEG and in terminal CH_2 group of PEG were around 3.64 ppm (b) and 4.36 ppm (c), respectively. The evidence for methene in GA occurred at around 4.8 ppm (d).

The infrared spectra of PEG, GA, D,L-LA and PLGA-PEG-PLGA were presented in Fig. 3. The peak at 1455 and 1352 cm^{-1}, similar to site of D,L-LA methyl group peak, were assigned to the characteristic of polymer's methyl group. The peaks at 2877 cm^{-1} and 1100 cm^{-1} were shown for the characteristics of polymer's methylene group near to oxygen atom and C–O–C group. So, it is proven that PEG ether linkage exists in the polymer. The peak at 1757 cm^{-1}, similar to site of D,L-LA and GA carbonyl group, represented for carbonyl group in polymer. The peak at 3497 cm^{-1} was attributed to terminal hydroxyl group of LA or GA structure piece in the polymer product, while the peak at 1189 cm^{-1} for C–O linkage of ester in polymer. Therefore, it could be concluded that in polymer there existed ester groups which were formed by inducting LA and GA into PEG. These results confirmed that PEG reacted with LA and GA, as a result, PLGA-PEG-PLGA was produced.

The molecular weight of copolymer was determined using GPC method. Chromatogram of copolymer was shown in Fig. 4. The elution volume was 28 mL for copolymers according to its molecular weight. The other peaks in the chromatogram were related to the solvents. The Mn (Number-average molecular weight), Mw (Weight-average molecular weight) and Mp (Peak molecular weight) of PLGA-PEG-PLGA were 7956, 9637 and 9912, respectively. The Pd (Polydispersity, Pd = Mw/Mn) of copolymer was about 1.233, which showed a symmetric peak and had a relative narrow molecular weight. Unimodal GPC with low polydispersity confirmed the formation of triblock copolymer.

3.2. Physicochemical characterization of copolymer micelles

3.2.1. CMC of copolymer

PLGA-PEG-PLGA copolymer in water can self-assemble into micelles. Figs. 5 and 6 showed that the CMC of copolymer at room temperature was 2.82×10^{-5} g/mL. The low CMC indicated that nano-scoped micelles could be formed at a lower copolymer concentration due to the strong hydrophobicity of PLGA-PEG-PLGA copolymer.

3.2.2. Particle size, zeta potential and morphology

The distribution of sizes of CUR-loaded micelles was shown in Fig. 7. The zeta potential of CUR-loaded micelles was about

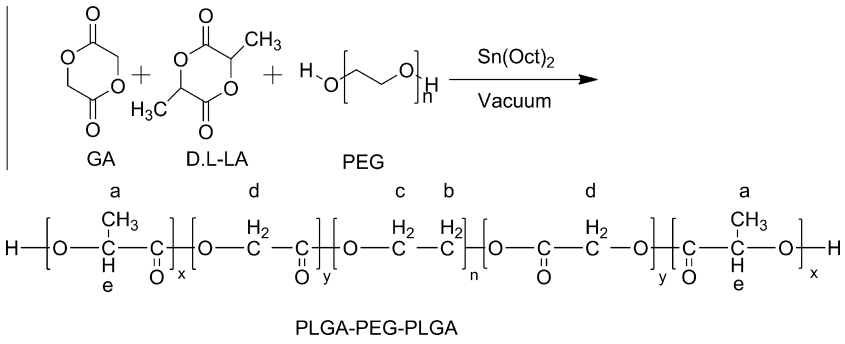

Fig. 2. The synthesis routine of PLGA-PEG-PLGA.

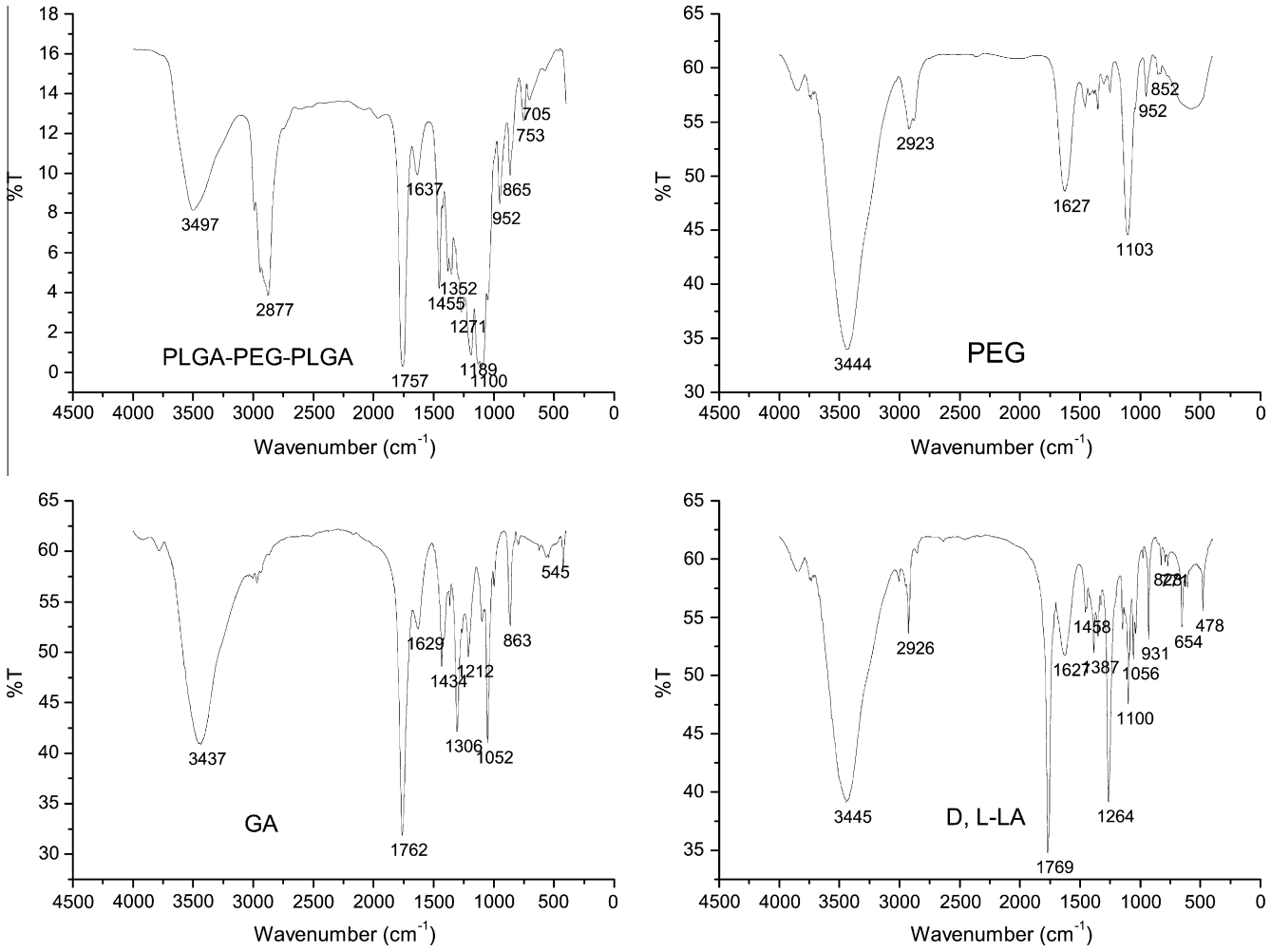

Fig. 3. IR spectrum of PLGA-PEG-PLGA, GA, D,L-LA and PEG.

−0.71 mV, which implied a nearly neutral surface charge. The average size of blank and CUR-loaded micelles was 24.74 nm and 26.29 nm with rather narrow size distribution patterns, respectively.

As shown in Fig. 8, the morphology of the CUR-loaded micelles observed under TEM was spherical in shape with a smooth surface.

3.2.3. Entrapment efficiency (EE) and drug loading (DL)

The average drug encapsulating efficiency and drug loading were 70 ± 0.34% and 6.4 ± 0.02% (w/w), respectively. The higher ratio of hydrophobic groups (such as GA and D,L-LA) in the core of PLGA-PEG-PLGA micelles made CUR more easily load into the core of PLGA-PEG-PLGA micelles by interaction between CUR and hydrophobic group of PLGA-PEG-PLGA micelles. So, this high EE and DL were considered as a result of the synergistic effect of the unique micellar encapsulation.

3.3. Evaluation of the pharmacokinetics of micelles following i.v. administration

Because of PLGA-PEG-PLGA's degradation described in the early report [39], CUR in tissues was extracted with acetic ether as soon

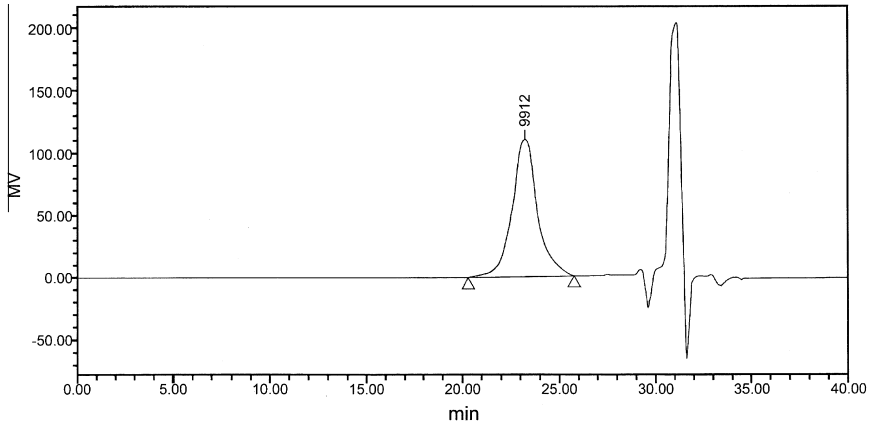

Fig. 4. Gel permeation chromatograms of PLGA-PEG-PLGA.

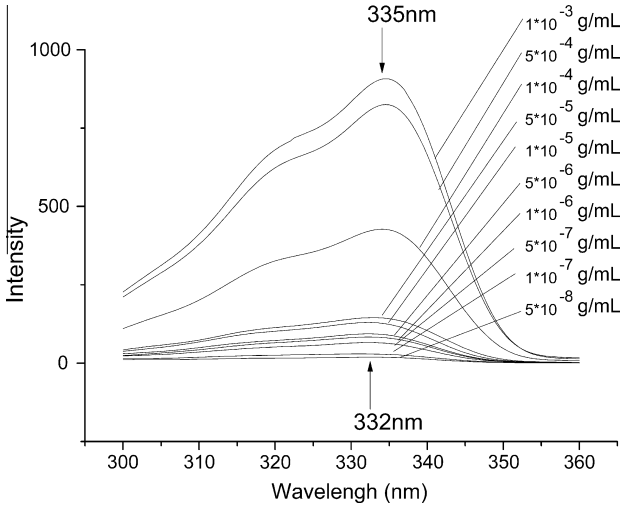

Fig. 5. Pyrene excitation spectra of PLGA-PEG-PLGA aqueous solutions (emission wavelength at 390 nm).

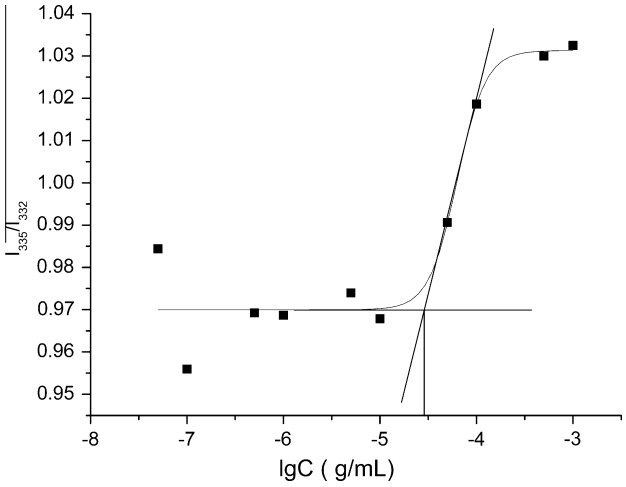

Fig. 6. Intensity ratio of I_{335}/I_{332} vs. lgC for PLGA-PEG-PLGA in water.

as possible in sample preparation for analysis of HPLC in order to avoid degradation. Citric acid (pH = 3.0) was added to keep stability of CUR because CUR was stable only in acid environment (pH = 3.0–6.5) [40]. The chromatograms of CUR showed a stable baseline and good resolution between CUR and endogenous materials in plasma and tissues. The limit of detection found was 10 ng/mL and the mean recovery of CUR in plasma and tissues was more than 80% within the range of 20–1000 ng/mL at the present assay conditions.

The profiles of CUR concentration in plasma *vs.* time were shown in Fig. 9, CUR from both formulations was eliminated in vivo in a short time, and the concentration of CUR in plasma was lower than 10 ng/mL at 4 h after administration.

Based on the analysis of the models and parameters with "DAS2.0 practical pharmacokinetics program", it was concluded that the in vivo pharmacokinetics of CUR-loaded micelles in blood could be described by two-compartment model after i.v. administration. The pharmacokinetic parameters, such as area under the drug concentration–time curve values ($AUC_{(0-\infty)}$), mean residence time (MRT), total clearance ($CL/_Z$), and biological half life ($t_{1/2\alpha}$, $t_{1/2\beta}$), were reported in Table 1.

As shown in Table 1, the pharmacokinetic parameters of CUR micelles in mice showed significant changes in comparison to these of the CUR solution. PLGA-PEG-PLGA micelles provided higher $AUC_{(0-\infty)}$ (1.31 fold), MRT (2.67 fold), clearance half life ($t_{1/2}$) (2.48 fold) and distribution half life ($t_{1/2}$) (4.54 fold) compared to the CUR solution. The CUR-loaded micelles also decreased $CL/_Z$ and C_{max} compared to CUR solution, respectively. The prolongation of half life ($t_{1/2}$), enhanced residence time (MRT) and decreased total clearance ($CL/_Z$) indicated that CUR-loaded micelles could prolong acting time of CUR in vivo. This result may be related to the CUR location within the micelles and increased viscosity of copolymer solution at the body temperature [14]. The variation of $AUC_{(0-\infty)}$ from 474.0 ± 18.21 μg/L h to 621.6 ± 24.68 μg/L h indicated that the CUR-loaded micelles provided higher bioavailability than CUR solution.

3.4. Evaluation of biodistribution of micelles in mice following i.v. administration

The tissue distribution of CUR micelle and CUR solution after intravenous administration was compared in mice. As shown in Fig. 10 and Fig. 11, CUR was widely and rapidly distributed into most tissues with exception of heart following i.v. administration of micellar preparation. Micelles could markedly promote enrichment of CUR in lung, brain and kidney and reduce the distribution of CUR in spleen and liver compared with CUR solution. The results indicated that the CUR micelles could deliver CUR mainly to kidney and lung at 5 min. Drug concentrations for CUR micelles attached to peak concentration in liver (2214.9 ng/g) and kidney (426.9 ng/g) at this time. After 30 min, the drug was not detected in

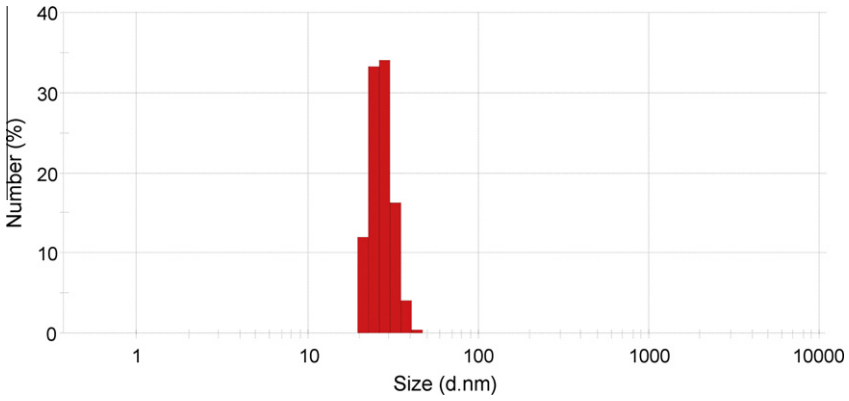

Fig. 7. Distribution of copolymer's micelle size.

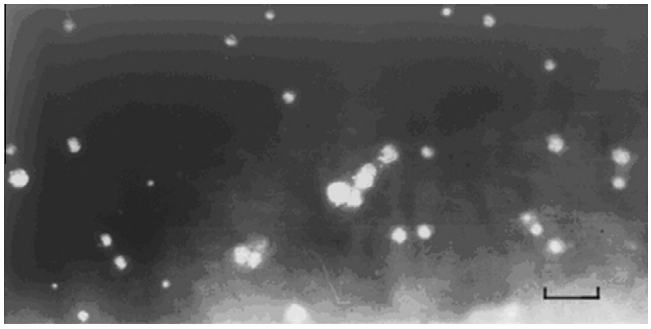

Fig. 8. TEM micrograph of CUR-loaded micelles (100,000×, the scale bar is 100 nm).

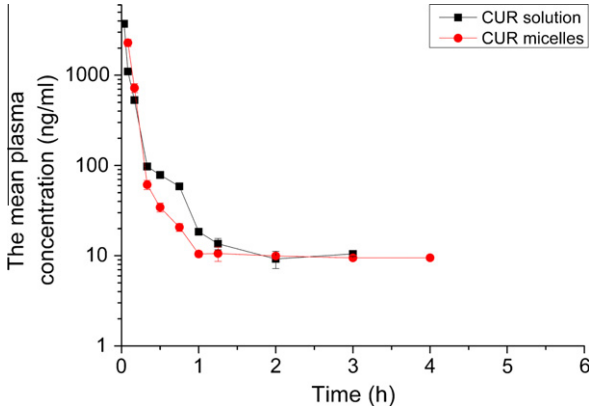

Fig. 9. The profile of concentration of CUR in plasma verse time after i.v. injection of CUR solution and CUR micelles.

Table 1
The pharmacokinetic parameters of CUR solution and CUR micelles ($n = 5$).

Pharmacokinetic parameters	CUR solution	CUR micelles
$t_{1/2\alpha}$ (h)	0.023 ± 0.005	0.057 ± 0.001
$t_{1/2\beta}$ (h)	0.254 ± 0.075	1.153 ± 0.083
$AUC_{(0-\infty)}$ (μg/L h)	474.0 ± 18.21	621.6 ± 24.68
$MRT_{(0-\infty)}$ (h)	0.338 ± 0.027	0.901 ± 0.107
C_{max} (mg/L)	3.661 ± 0.049	2.173 ± 0.099
$CL/_Z$ (L/h/kg)	21.119 ± 0.827	16.107 ± 0.66

kidney. While the drug concentrations in lung for micelles showed the gradually decreased trend with time up to 24 h. In brain, at 4 h after administration drug concentrations for micelles reached peak

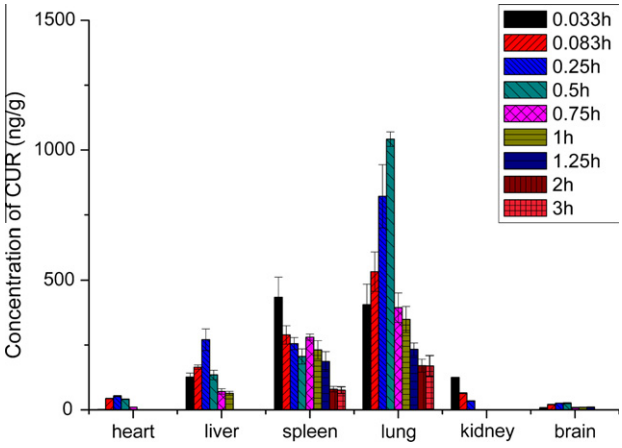

Fig. 10. Distribution in tissue in mice after i.v. administration of CUR solution.

value (161.9 ng/g) which was 6.28 folds that (25.8 ng/g) for CUR solution. This result demonstrated that PLGA-PEG-PLGA micelles could distinctly enhance distribution of drug into brain.

It was noted that the diameter of 26 nm for the PLGA-PEG-PLGA micelles was consistent with a model of spherical single core micelle reported in early research [41,42], in which the condensed PLGA core is surrounded by a shell of PEG strands. The advantage of a small diameter as well as distinct core–shell architecture contributed substantially to the reduced uptake into the reticuloendothelial system in liver and spleen.

In the early report, it was demonstrated that the blood–brain barrier (BBB) might be overcome by particles with a size of about <50 nm [43]. The surface charge of nanoparticles was also an important feature in their effectiveness, because neutral or negatively charged surfaces experienced a greater volume of distribution when directly delivered in brain [44]. So, it was concluded that the smaller diameter (26 nm) and the nearly neutrally charged property (−0.71 mv for zeta potential) of CUR-loaded PLGA-PEG-PLGA micelles can contribute to the breakthrough of BBB and accumulation of drug in brain.

However, why could PLGA-PEG-PLGA micelles obviously elevate drug accumulation in lung? Nanocarriers about 100 nm in diameter are able to pass through the vascular endothelium and reach pulmonary alveoli [45]. Therefore, PLGA-PEG-PLGA micelles with a size of about 26 nm showed most potential for accumulation in the lungs. The pulmonary accumulation effect is also related to the physiological structure and function of the lungs. In order to cope with periods of high cardiac output and satisfy oxygen demands, blood pressure and the rate of perfusion in the lungs

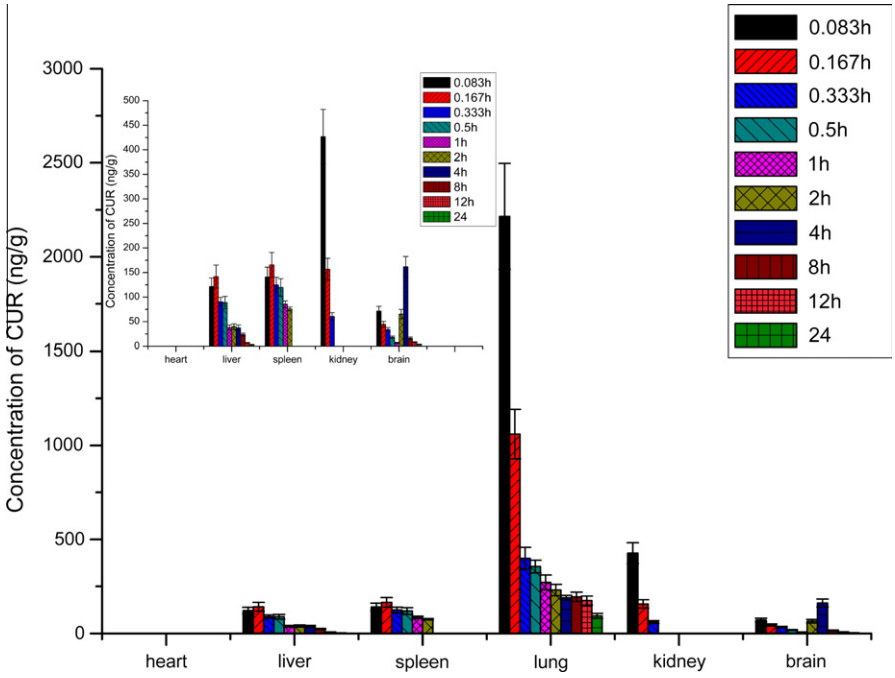

Fig. 11. Distribution in tissue of CUR in mice after i.v. administration of micelle preparation.

Table 2
Biodistribution indexes of CUR micelles and CUR solution in mice.

Tissue	CUR micelles		CUR solution		Ce[a]
	$AUC_{(0-\infty)}$ (μg/L h)	C_{max} (μg/L)	$AUC_{(0-\infty)}$ (μg/L h)	C_{max} (μg/L)	
Liver	546.09	141.68	142.02	270.61	0.52
Spleen	213.70	165.64	621.80	389.17	0.43
Lung	6922.8	1060.0	1245.6	1041.7	1.02
Heart	–	–	–	–	
Kidney	–	–	–	–	
Brain	853.71	161.87	59.65	80.73	2.00

[a] $Ce = (C_{max})_{micelles}/(C_{max})_{solution}$.

are significantly lower than in the systemic vasculature [46], which lays the foundation for the lung to receive high doses of injected drugs. Moreover, reports have indicated that the pulmonary accumulation of nanoparticles is caused by the selective absorption by pneumocytes [47]. The alveolar epithelium is formed by types I and II pneumocytes, and phospholipids and other pulmonary surfactants are synthesized and secreted by type II pneumocytes to degrade alveolar surface tension. The surfactant can be transported and suffers pinocytosis by type I pneumocytes [48]. The ability of PLGA-PEG-PLGA copolymer forming micelles indicated that it could present surface activity. The surface activity of PLGA-PEG-PLGA micelles could stimulate the adsorption of type I pneumocytes, and transfer CUR into the lungs. As a result, CUR accumulation was elevated in lung.

Ce is an index for distribution difference in tissues compared to the control [49]. It demonstrates the micelles' ability of changing drug's distribution in tissues. The larger its value is, the more obvious distribution difference is. The Ce values of CUR-loaded PLGA-PEG-PLGA micelles for brain and lung were respectively 2.00 and 1.02 (Table 2). These results showed that these micelles could obviously elevate the distribution of CUR in brain and lung. However, the Ce values for other tissues were less than 1. This result indicated that micelles decreased CUR's distribution in these tissues.

At many predetermined time points, the concentrations of CUR in heart and kidney for micelles and solution were lower than the assaying limit for CUR, therefore, many pharmacokinetic parameters could not be obtained, which indicated that CUR couldn't do harm to kidney and heart.

4. Conclusions

PLGA–PEG–PLGA triblock copolymers were synthesized by a ring-opening reaction of L-lactide with PEG using stannous octanate as catalyst. Micelles were firstly prepared with this triblock copolymers using solvent-dialysis method and successfully encapsulated hydrophobic CUR. The plasma $AUC_{(0-\infty)}$, $t_{1/2\alpha}$, $t_{1/2\beta}$ and MRT of CUR micelles in mice were improved compared to the control CUR solution, respectively. The biodistribution study in mice showed that the PLGA-PEG-PLGA micelle formulation decreased drug uptake by the liver and spleen, and increased the distribution of drug in lung and brain. The results implied that PLGA–PEG–PLGA micelles could be a promising drug carrier for water poorly soluble drug.

Reference

[1] N. Nishiyama, K. Kataoka, Pharmacol. Ther. 112 (2006) 630.
[2] V.P. Torchilin, Pharm. Res. 24 (2007) 1.
[3] M.C. Jones, J.C. Leroux, Eur. J. Pharm. Biopharm. 48 (1999) 10.
[4] G.S. Kwon, Crit. Rev. Ther. Drug Carr. Syst. 20 (2003) 357.
[5] H. Maeda, J. Wu, T. Sawa, Y. Matsumura, K. Hori, J. Controlled Release 65 (2000) 271.
[6] W.Y. Seow, J.M. Xue, Y.Y. Yang, Biomaterials 28 (2007) 1730.

[7] Y.N. Xue, Z.Z. Huang, J.T. Zhang, M. Liu, M. Zhang, S.W. Huang, R.X. Zhuo, Polymer 50 (2009) 3706.
[8] K.T. Oh, Y.T. Oh, N.M. Oh, K. Kim, D.H. Lee, E.S. Lee, Int. J. Pharm. 375 (2009) 163.
[9] R.J. Laporte, Hydrophilic Polymer Coatings for Medical Devices: Structure/Properties, Development, Manufacture, and Applications, Technomic Publishing Co., Lancaster, PA, 1997. p. 57.
[10] D.E. Owens, NA Int. J. Pharm. 307 (2006) 93.
[11] A. Vonarbourg, C. Passirani, P. Saulnier, J.P. Benoit, Biomaterials 27 (2006) 4356.
[12] G.M. Zentner, R. Rathi, C. Shih, J.C. McRea, M.H. Seo, H. Oh, B.G. Rhee, J. Mestecky, Z. Moldoveanu, M. Morgan, S. Weitman, J. Controlled Release 72 (2001) 203.
[13] S.B. Chen, R. Pieper, D.C. Webster, J. Singh, Int. J. Pharm. 288 (2005) 207.
[14] A.A. Ghahremankhani, F. Dorkoosh, R. Dinarvand, Polym. Bull. 59 (2007) 637.
[15] S.B. Chen, J. Singh, Int. J. Pharm. 352 (2008) 58.
[16] Y.M. Kwon, S.W. Kim, Pharm. Res. 21 (2004) 339.
[17] C. Pratoomsoot, H. Tanioka, K. Hori, S. Kawasaki, S. Kinoshita, P. Tighe, J.H. Dua, K.M. Shakesheff, F.R.A.J. Rose, Biomaterials 29 (2008) 272.
[18] J.H. Jeong, S.W. Kim, T.G. Park, Pharm. Res. 1 (2004) 50.
[19] Z. Gao, A.N. Lukyanov, A. Singhal, V.P. Torchilin, Nano Lett. 2 (2002) 979.
[20] J.H. Lee, S.W. Jung, I.S. Kim, Y. Jeong, Y.H. Kim, S.H. Kim, Int. J. Pharm. 251 (2003) 23.
[21] I.S. Kim, S.H. Kim, Int. J. Pharm. 226 (2001) 23.
[22] C. Kim, S.C. Lee, S.W. Kang, I.C. Kwon, Y. Kim, S.Y. Jeong, Langmuir 16 (2000) 4792.
[23] R.K. Maheshwari, A.K. Singh, J. Gaddipati, R.C. Srimal, Life Sci. 78 (2006) 2081.
[24] K. Ono, K. Hasegawa, H. Naike, M. Yamada, J. Neurosci. Res. 75 (2004) 742.
[25] B.B. Aggarwal, A. Kumar, A.C. Bharti, Anticancer Res. 23 (2003) 363.
[26] H. Hatcher, H. Planalp, J. Cho, F.M. Torti, S.V. Torti, Cell. Mol. Life Sci. 65 (2008) 1631.
[27] K. Letchford, R. Liggins, H. Burt, J. Pharm. Sci. 97 (2008) 1179.
[28] P. Anand, A.B. Kunnumakkara, R.A. Newman, B.B. Aggarwal, Mol. Pharmacol. 4 (2007) 807.
[29] A. Sahu, U. Bora, N. Kasoju, P. Goswami, Acta Biomater. 4 (2008) 1752.
[30] Z. Ma, A. Haddadi, O. Molavi, A. Lavasanifar, R. Lai, J. Samuel, J. Biomed. Mater. Res., Part A 86 (2008) 300.
[31] L. Li, B. Ahmed, K. Mehta, R. Kurzrock, Mol. Cancer Ther. 6 (2007) 1276.
[32] S. Bisht, G. Feldmann, S. Soni, R. Ravi, C. Karikar, A. Maitra, J. Nanobiotechnol. 5 (2007) 3.
[33] K. Sou, S. Inenaga, S. Takeoka, E. Tsuchida, Int. J. Pharm. 352 (2008) 287.
[34] P.K. Vemula, J. Li, G. John, J. Am. Chem. Soc. 128 (2006) 8932.
[35] A.G. Ali, D. Farid, D. Rassoul, Polym. Bull. 59 (2007) 637.
[36] Q.Z. Lv, A.H. Yu, Y.W. Xi, H.L. Li, Z.M. Song, J. Cui, F.L. Cao, G.X. Zhai, Int. J. Pharm. 372 (2009) 191.
[37] Z.S. Ma, S. Anooshirvan, R.B. Dion, A. Lavasanifar, J. Samuel, Biomed. Chromatogr. 21 (2007) 546.
[38] S. Chen, J. Singh, Int. J. Pharm. 295 (2005) 183.
[39] M.X. Qiao, D.W. Chen, X.C. Ma, Y.J. Liu, Int. J. Pharm. 294 (2005) 103.
[40] L. Yu, Z. Zhang, H. Zhang, J.D. Ding, Biomacromolecules 10 (2009) 1547.
[41] C. Tanford, Y. Nozaki, M.F. Rohde, J. Phys. Chem. 81 (1977) 1555.
[42] R. Xu, M.A. Winnik, F.R. Hallett, G. Riess, M.D. Croucher, Macromolecules 24 (1991) 87.
[43] R.G. Thorne, C. Nicholson, Proc. Natl. Acad. Sci. 103 (2006) 5567.
[44] J.A. MacKay, D.F. Deen, F.C. Szoka Jr., Brain Res. 1035 (2005) 139.
[45] M. Smola, T. Vandamme, A. Sokolowski, Int. J. Nanomedicine 3 (2008) 1.
[46] T. Dziubla, V. Muzukantov, in: V.P. Torchilin (Ed.), Nanoparticulates as Drug Carriers, Imperial College Press, London, 2006, p. 499.
[47] Q.Y. Xiang, M.T. Wang, F. Chen, T. Gong, Y.L. Jian, Z.R. Zhang, Y. Huang, Arch. Pharm. Res. 40 (2007) 519.
[48] A.G. Serrano, J. Perez-Gil, Chem. Phys. Lipids 141 (2006) 105.
[49] M. Yamaguchi, K. Ueda, A. Isowaki, A. Ohtori, H. Takeuchi, N. Ohguro, K. Tojo, Biol. Pharm. Bull. 32 (2009) 1266.